VOL. 15, NO. 11, JUNE 2020 ISSN 1819-6608
ARPN Journal of Engineering and Applied Sciences

www.arpnjournals.com

IMPROVING THE SHIELD MACHINE CUTTER HEAD FOR TUNNELING UNDER THE CONDITIONS OF THE METROSTROY SAINT PETERSBURG MINES

Dmitrii A. Yungmeister, Sergey A. Lavrenko, Aleksey I. Yacheikin and Rustam Yu. Urazbakhtin
Department of Engineering, Saint-Petersburg Mining University, Russian Federation
E-Mail: Lavrenko_SA@pers.spmi.ru

ABSTRACT

The paper considers the specifics of tunneling in the complicated geological conditions of the Metrostroy Saint Petersburg mines using the Herrenknecht S-782 shield machine. The techniques for defining the cutting force in the tool face have been analyzed. The dependence of the total torque of the shield machine cutter head shaft has been plotted. An option of the cutter lacing pattern on the rotary cutter head of the shield machine has been proposed.

Keywords: shield machine, lacing pattern, clay, chip thickness, cutting force.

INTRODUCTION

The metro is the most popular and complicated in terms of construction municipal transportation hub. Its popularity is due to the speed and ease of human traffic.

The Saint Petersburg Metro is constructed in complicated geological conditions. Tunneling is performed at a depth of 15 to 70 m. At shallow depths, the rocks are mainly represented by clays with inclusions of granite boulders and pebbles, however, interbeds of limestone and sandstone occur with depth (Figure-1). At a depth of more than 50 meters, only clays occur [1].

Figure-1. Sandstone interbeds in the clay rock; granite boulder and pebble inclusions.

The subway construction is accompanied by vertical shafting, building shaft bottoms with service roadways, mainline tunneling, and building stations [2]. To do that, a set of machines is used, including the shaft sinking combine SPK-6, shield machines KT1-5,6 [3], Herrenknecht S-782 (Figure-2), and Herrenknecht S-441 (for inclined tunneling) [4], and special tubbing erectors to drive short special-purpose tunnels [5]. The Herrenknecht S-782 and S-441 shield machines are the most modern ones [6].

Figure-2. The Herrenknecht S-782 shield machine.

The Herrenknecht S-782 tunnel-boring mechanized complex (TBMC) is a shield machine with earth pressure balance designed to drive two-track tunnels with a diameter of 10.5 meters in complicated geological conditions [7]. The rotary cutter head is equipped with rock-breaking tools - cutting knives and disk roller-type cutters [8].

Like tunneling, the installation of the modern Herrenknecht TBMC starts with sinking an entry pit with a depth of about 15 meters. Further, the tunnel depth increases with its length. Upon the tunneling completion, the TBMC arrives in a dismantling chamber located in homogeneous rocks at a depth of 50-60 meters.

The practice of using the Herrenknecht S-782 shield machine showed the insufficient efficiency of its cutter head in an inhomogeneous cut face rock (clay with solid inclusions), which is explained by the high wear of rock-breaking tools. When tunneling through homogeneous clay, an increased power intensity of the cut face rock destruction and a low tunneling rate due to the lacing pattern corresponding to the full-face driving have been revealed.

EXPERIMENTAL STUDIES OF CLAY DESTRUCTION BY CUTTING

To study the single-cutter clay destruction, experimental studies have been conducted at the laboratory bench of the Mechanical Engineering Department of the Mining University (Figure-3).

Figure-3. Bench for studying single-cutter Cambrian clay cutting.

1 - moving traverse; 2 - suspension grip; 3 - rod; 4 - cutting knife; 5 - clamps; 6 - measuring transducer; 7 - guiding bars; 8 - tool holder; 9 - adjustment screw; 10 - table with a clamping device to fix a Cambrian clay sample; 11 - fixed traverse

Fragments of argillite-like thin-layered clay of the Kotlin horizon were used as samples. The locked cuts were executed from a leveled surface. The chip thickness was 10, 15, and 20 mm. The cuts were made across the bedding. After each cut, the destruction products were collected and weighed, the shapes of the large chip elements analyzed, and the fracture surfaces studied.

The similarity of the single-cutter clay fragment destruction to the stationary process was estimated based on the cutting force probability density function plot. The required confidence factor of the experimental results was assumed to be 0.95 at a relative measurement error of 0.05. The Cambrian clay cutting power and energy parameters were analyzed using five oscillograms obtained under the same conditions.

The study of cut surfaces in the Cambrian clay samples and the shape of large chips allowed finding the following dependencies.

It is known that the brittle rock cutting is cyclical and accompanied by the rock fragmentation, forming a compaction core from fine dust, and splitting successive chip elements off the rock mass. The Cambrian clay destruction in the form of thin chips ($h \leq 15$ mm) is similar to cutting brittle rocks. The chips are well-defined and split off the rock mass by semicircular separation cracks. The lateral fracturing occurs almost over the entire cut depth (Figure-4a). The lower cut surface is uneven and characterized by numerous induced defects and discontinuities.

With increasing chip thickness, the cross-sectional shape of cuts in the clay samples changes. The cut bottom and the side surfaces intersect at almost a right angle, the cut does not fracture to the full depth (Figure-4a). Large elements split off the rock mass with the formation of shear cracks, the development of which is accompanied by significant plastic rock deformation. Thus, a significant part of the power supplied to the rock-breaking tool is spent on overcoming the inelastic deformation energy of the clay mass and not on the formation of new fracture surfaces, which negatively affects the specific power consumption of cutting.

(a)

ARPN Journal of Engineering and Applied Sciences

www.arpnjournals.com

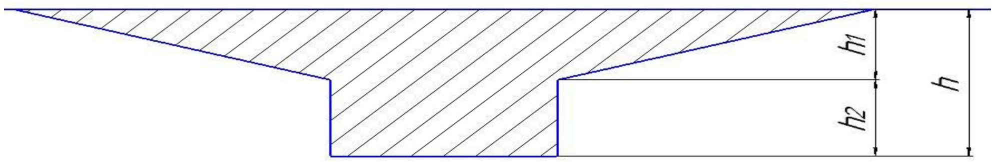

(b)

Figure-4. The cut surface structures when single-cutter destructing the Cambrian clay samples: a) the structure of the clay fracture surface after the cutting; b) graphical interpretation of the clay fracture surface structure.

The plastic deformation magnitude has been determined by the Cambrian clay sample natural moisture content, the cutting pattern, and the geometric parameters of the rock-breaking tool. In the course of laboratory experiments, it has been found that on the flat front edge of the cutter used, a dense sticky fine dust builds up that reduces the cutting angle and does not destroy during subsequent cuts. The cutter gumming negatively affects the performance of tunnel shields and increases the load on the mining machine drive elements [16].

To optimize the clay cutting, it is required to achieve cleavage or brittle cutting.

As can be seen from Figures 4a and 4b, destruction of clay by a cutter can be conditionally divided into two phases – forming the brittle (h_1) and ductile (h_2) chips, since the bottom surface of the cutting groove remains straight and its magnitude at the parameters specified is 4-5 mm and increases with increasing the chip thickness.

CALCULATING THE DEPENDENCE OF THE ROCK-BREAKING TOOL CUTTING FORCE USING VARIOUS TECHNIQUES

The thickness of the chips cut off by the rotary cutter head is proportional to the velocity of its travel to the cut face and can be determined by the formula:

$$h = \frac{v_n}{n_{uo} \cdot m},$$

where m is the number of cutters in a cutting line (according to the technical documents, in total, the rotor has 103 cutters installed, of which 56, 38, and 9 cutters are banked in cutting lines of 4, 2, and 1, respectively); v_t is a velocity of the cutter head travel to the cut face, m/s; n_{ch} is the cutter head rotation frequency, s^{-1}.

$h_1 = \frac{0{,}0005\ \text{m/s}}{0{,}025c^{-1} \cdot 1} = 20$ mm; $h_2 = \frac{0{,}0005\ \text{m/s}}{0{,}025c^{-1} \cdot 2} = 10$ mm; $h_4 = \frac{0{,}0005\ \text{m/s}}{0{,}025c^{-1} \cdot 4} = 5$ mm.

The rock hardness ratio according to the Protodyakonov scale is within a large interval of 1 to 15 (1 - clay, 15 - granite boulders) due to the cut face diversity. Destruction of rocks by cutting is possible within the interval $f = 1 \div 4$.

The cutting force in the tool face can be calculated based on four techniques using different physical and mechanical rock properties such as the rock cutting strength A_c, the contact strength of the rock P_c, and the rock compressive strength σ_{comp} that can be determined by the following empirical dependencies:

$A_c = 150 \cdot f$, kN/m;
$P_c = 13 \cdot \sigma_{com}$, MPa [9];
$\sigma_{comp} = 2{,}4954 \cdot f^{1{,}789}$, MPa [10].

Technique No. 1. Defining the Cutting Force in the Cutter According to the Plough System Calculation Technique [11]

$$P_{zp} = 0{,}108 \cdot A_c \cdot \frac{1 + k_n \cdot f' \cdot (1 + 1{,}8 \cdot S) \cdot (0{,}35 \cdot b + 3)}{(0{,}45 \cdot h + b + 23) \cdot k_\psi \cdot \cos\beta} \cdot h \cdot t_{cut} \cdot k_a \cdot k_{pt} \cdot k_{sh} \cdot k_{sl} \cdot k_{cf},$$

where A_c is the average formation cutting strength, kN/m; k_n is a coefficient characterizing the ratio of the sloughing and cutting forces in a sharp cutter; f' is a cutting strength factor; S is the projection of the cutter worn place on the cutting plane, cm^2; b is the cutting edge width, mm; h is the chip thickness, mm; t_{cut} is a cut width, mm; k_a is a coefficient depending on the cutting angle; k_ψ is a coefficient considering the brittle-ductile coal properties; β is the cutter setting angle to the driving direction; k_{pt} is the cutting pattern factor; k_{sh} is the tool face shape factor; k_{sl} is the sloughing factor; k_{cf} is the cut face opening factor.

Table-1. Values of parameters and coefficients (Technique No. 1).

A_c, kN/m	b, mm	h, mm	t_{cut}, mm	t, mm	S, cm^2	f	k_a	k_ψ	β	k_{pt}	k_{sh}	k_{sl}	k_n	k_{cf}
91.6; 218.6; 323.9	100	10	100	100	4	0.4	1.24	0.85	0	1	0.9	0.67	0.85	0.47

Technique No. 2. Defining the Cutting Force in the Cutter According to the Shield Tunneling Machine Calculation Technique [2]

$$P_{zp} = P_k \cdot k_\alpha \cdot k_b \cdot (0,25 + 0,018 \cdot t \cdot h) + 0,27 \cdot \mu_\partial \cdot P_k \cdot F_{cp}$$
,

where P_c is the rock contact strength, MPa; k_α is a coefficient considering the effect of the cutting angle; $\mu_д$ is the coefficient of the cutter friction on the rock; F_{av} is the average projection of the cutter worn place along the back edge on the cutting plane, mm^2, t is the cutter pitch, mm; *b* is the cutting edge width, mm; k_b is a coefficient considering the effect of the cutting edge width.

Table-2. Values of parameters and coefficients (Technique No. 2).

P_c, MPa	b, mm	h, mm	t, mm	F_{av}, mm^2	k_α	k_b	μ_∂
13; 59; 113	100	10	100	100	1	1.92	0.4

Technique No. 3. Defining the Cutting Force in the Cutter According to the Boom Miner Calculation Technique RD 12.25.137-89 [13]

$$P_{zp} = P_k \cdot (k_T \cdot k_G \cdot k_\alpha \cdot (0,25 + 0,018 \cdot t \cdot h) + 0,1 \cdot F_{av},$$

where k_T is a coefficient considering the cutter type effect; k_G is a coefficient considering the tool geometry effect.

Table-3. Values of parameters and coefficients (Technique No. 3).

P_c, MPa	b, mm	h, mm	t, mm	F_{av}, mm^2	k_α	k_T	k_G
13; 59; 113	100	10	100	100	1	1	1.92

Technique No. 3. Defining the Cutting Force in the Cutter According to the Institute of Mining Technique (A.A. Skochinsky Institute of Mining) [14]

$$P_{zp} = 98,1 \cdot \bar{A} \cdot \frac{0,35 \cdot b + 0,003}{k_\varphi (b + h_{cut} \cdot tg\phi)} \cdot t_{cut} \cdot h_{cut} \cdot k_{cf} \cdot k_a \cdot k_{sl} \cdot k_{sh} \frac{1}{\cos\beta},$$

Where k_φ is a coefficient considering the effect of brittle and ductile coal properties.

Table-4. Values of parameters and coefficients (Technique No. 4).

A_c, kN/m	*h, m*	*b, m*	*t, m*	k_φ	k_{sh}	k_a	k_{sl}	β	k_{cf}	$tg\phi$
91.6; 218.6; 323.9	0.01	0.1	0.1	0.85	0.9	1.24	0.67	0	0.54	0.68

After calculating the cutting force in the tool face according to four techniques and bringing them to a single physical and mechanical property - the compressive strength of the rock, we obtained a graph (Figure-5).

VOL. 15, NO. 11, JUNE 2020 ISSN 1819-6608
ARPN Journal of Engineering and Applied Sciences

www.arpnjournals.com

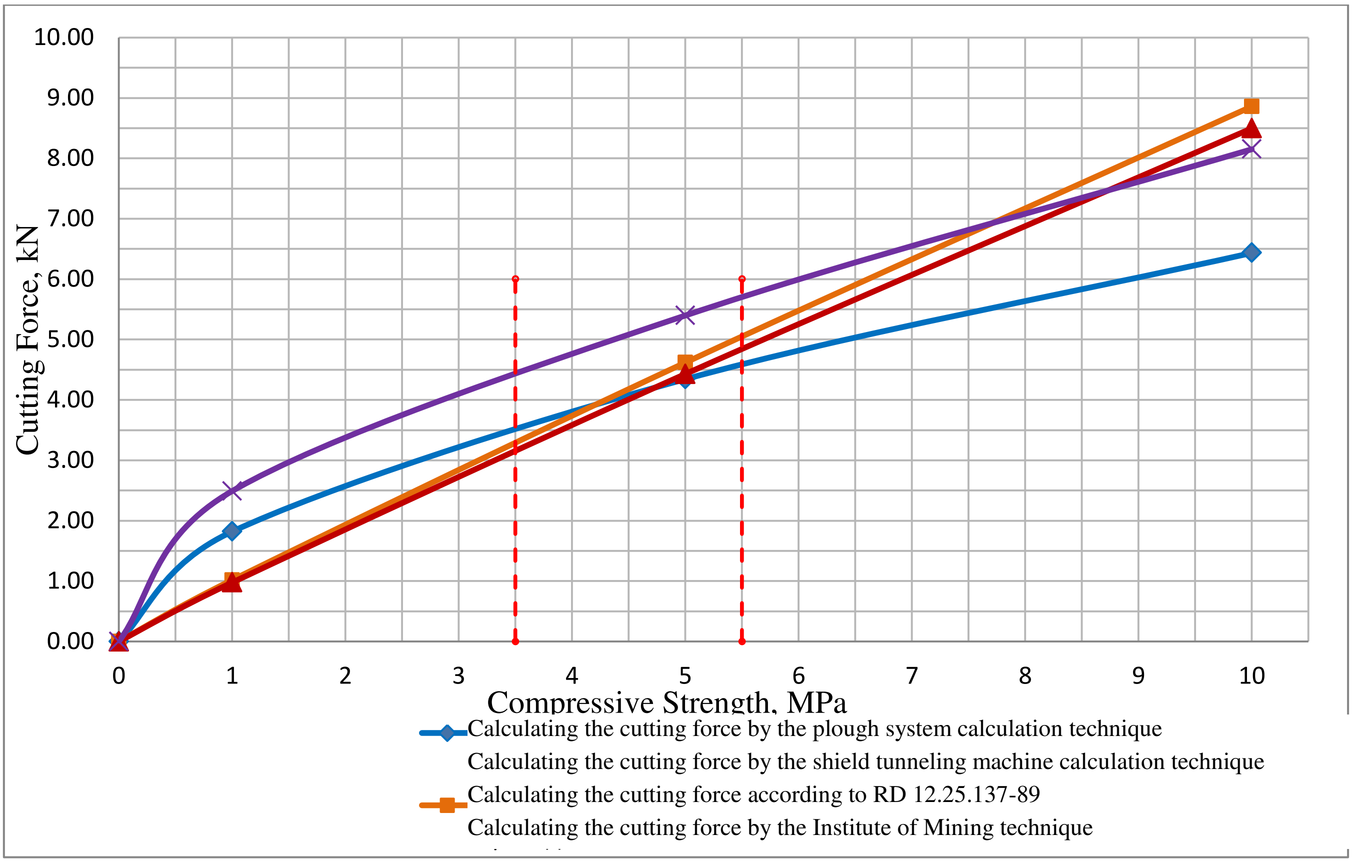

Figure-5. Dependence of the cutting force in the tool face on the compressive strength of the rock analysis of the tool face cutting force calculations results based on different techniques.

Having analyzed the graph (Figure-5), we can conclude that at σ_{comp}< 4 MPa, techniques No. 1 and No. 4 give an overestimated tool face cutting force value and at σ_{comp} > 4 MPa and σ_{comp} > 8 MPa, technique No. 1 and technique No. 4 give an underestimated tool face cutting force value, respectively, which indicates the impossibility of using these techniques in the calculations of strong rocks. Herewith, within 3.5 < σ_{comp} < 4.5 that corresponds to the Upper-Kotlin clay compressive strength, techniques No. 1 and No. 3 gave approximately the same tool face cutting force values. In further calculations, technique No. 2 - by the shield tunneling machine calculation technique will be applied

TORQUE CALCULATION

The torque required to destroy the cut face rock with a cutting tool has been calculation by to the following relationship:

$$M_{pi} = P_{z_{p\,i}} \cdot n_i \cdot R_{avi},$$

where $P_{z_{p\,i}}$ is the force in the cutter in a cutter pattern band, kN·m; n_i is the number of cutters in a cutter pattern band ($n_1 = 9$; $n_2 = 38$; $n_4 = 56$); R_{avi} is the average cutter bands pattern radius (for a cutter pattern band with one, two, and four cutters in a line, R_{avi} = 1.1, 2.5, and 4.15 m, respectively (Figure-6)).

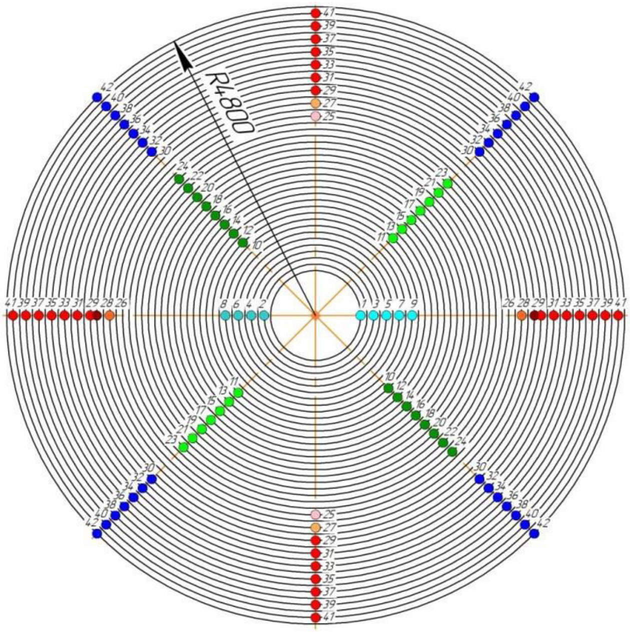

Figure-6. The Herrenknecht S-782 TBMC rotary head cutting pattern.

To obtain the total torque, the individual cutter pattern band torques should be summarized:

ARPN Journal of Engineering and Applied Sciences

$$\sum M_p = M_{p1} + M_{p2} + M_{p4}.$$

In a similar way, the cutting forces and torques required to destroy the cut face rock by jumpers and buckets are calculated.

CALCULATING FORCES AND TORQUE IN A ROLLER-TYPE ROCK-BREAKING TOOL

The disk cutter rolling force is calculated according to the technique by Rostami J. and Ozdemir L. [15]:

$$P_z = \frac{2{,}12 \cdot \sqrt[3]{\frac{s\sigma_{comp}^2 \sigma_t}{\gamma\sqrt{RT}}} RT\gamma}{1+\psi} \sin\frac{\gamma}{2};$$

where s is the cutting pitch, mm; σ_{comp} is the rock compressive strength, MPa; σ_t is the rock tensile strength, MPa; R is the cutter disc radius, mm; T is the cutting edge width, mm; γ is the tool - rock contact angle, rad; ψ is a coefficient describing the distributed load function (it is within -0.2 to 0.2 and decreases with increasing the cutting edge width).

The roller-type rock-breaking tool torque is calculated by the following relationship:

$$M_r = P_z \cdot n \cdot R_{av},$$

where n is the number of roller-type cutters; R_{av} is the average cutting pattern radius, m.

Figure-7 shows the dependence of the total torque in the cutting knife and roller-type rock-breaking tool on the rock compressive strength. The graph shows a torque limit, which is 21 kN·m according to technical documents.

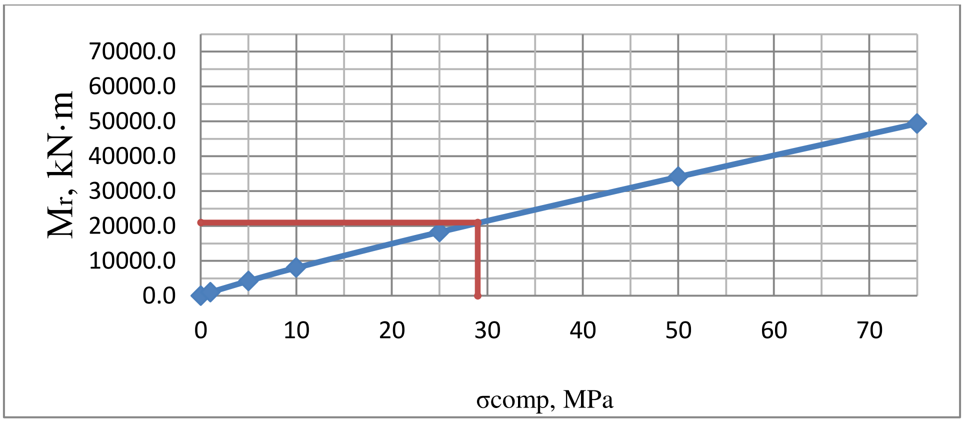

Figure-7. Dependence of the total torque in the rock-breaking tools on the rock compressive strength.

CONCLUSIONS AND RECOMMENDATIONS

The use of domestic RKS type cutters with a smaller cutting edge width combined with an increased lacing pitch (Figure-8b) as compared with the factory pattern (Figure-8a) allows improving the efficiency of clay cutting due to the increased cleavage width that will further lead to reduced power consumption of the cut face rock fracturing. In addition, due to the decreased width of the cutting edge, the torque in the cutters will decrease, which will further lead to the reduced TBMC power consumption.

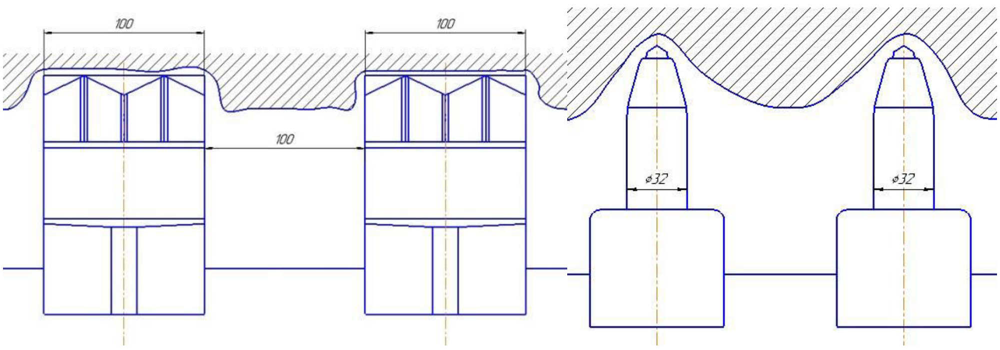

(a) (b)

Figure-8. The Cutter Head Cutting Pattern: a - factory cutting pattern; b- improved cutting pattern.

REFERENCE

[1] 2011. Peculiarities of Engineering Geological Conditions of Saint Petersburg / Dashko R. E., Aleksandrova O. Yu., Kotyukov P. V., Shidlovskaya A. V. // Urban Development and Geotechnical Construction. (1): 1-47.

[2] 1989. Construction of Tunnels and Subways / Golitsinsky D. M., Frolov Yu. S., Kulagin N. I., et al.; Ed. Golitsinsky D. M. - M.: Transport. p. 319.

[3] 2018. Improving the Work of the Cutter Head of the Tunnel Shield KT1-5.6M / Lukin D. G., Yungmeister D. A., Yacheykin A. I., Isaev A. I. // Mining Journal.

[4] 2017. Mining Machinery and Equipment. Underground Mining Machinery and Equipment: Educational-Methodical Complex / St. Petersburg Mining University. Comp. Yungmeister D. A. SPb. p. 117.

[5] 2014. Mechanized Complexes for Roadway Development at Mines of «Metrostroy» JSC (Saint Petersburg) / Verzhanskiy, A. P., Yungmeyster, D. A., Lavrenko, S. A., Isaev, A. I., Ivanov, A. V.// Gornyi Zhurnal.

[6] 2007. Tunneling Machinery Introducing a New Era in the Underground Transport Systems: Herrenknecht Tonnelservice Prosp. p. 20.

[7] 2013. Mechanized Tunneling in Urban Areas. Design Methodology and Construction Control / ed. Guglielmetti V., Grasso P., Makhtab A., Xu S.; Geodata S.p.A. Turin, Italy - St. Petersburg.: Polytechnic University Publishing House. p. 602.

[8] www.herrenknecht.com

[9] 1980. Defining Forces Acting on Rotary Cutters / Glatman L. B., Kekelidze Z. Sh., Yashina L. S. // Sc. Reports by A. A. Skochinsky Institute for Mining. 191: 85-90.

[10] 2003. Comparison of Rock Classifications by Strength / Tanayno A. S.- Bulletin of the Kuzbass State Technical University. 6(37).

[11] Lugantsev B. B. 2011. Calculation and Design of Plough Systems / Lugantsev B. B., Osherov B. A., Fainburd L. I., Averkin A. N.// - Moscow: Mining Book. p. 291.

[12] Shield Tunneling Machines / Brenner V. A., Zhabin A. B., Shchegolevsky M.M., *et al.* 2009. Moscow: Mining Book. p. 360.

[13] RD 12.25.137-89.

[14] OST 12.44.258-84. 1986. Selection of Parameters and Calculation of Forces for Cutting and Feed on Actuators. Procedure. - M.: Ministry of Coal Machine Building. p. 108.

[15] Rostami J., Ozdemir L. 1993. A New Model for Performance Prediction of Hard Rock TBMs // Rapid Excavation and Tunneling Conference: Proceedings. - Boston. pp. 793-809.

[16] Gabov V. V., Zadkov D. A., Nguyen Khac Linh. 2019. Features of elementary burst formation during cutting coals and isotropic materials with reference cutting tool of mining machines. Journal of Mining Institute. 236: 153-161. DOI: 10.31897/pmi.2019.2.153